

## Prediction of the color of dyes by using time-dependent density functional theory (TD-DFT)

S. Kawauchi<sup>1\*</sup>, L. Antonov<sup>1,2\*</sup>, Y. Okuno<sup>3</sup>

<sup>1</sup>Department of Organic and Polymeric Materials, Tokyo Institute of Technology, 2-12-1 O-okayama, Meguro-ku, 152-8552 Tokyo, Japan

<sup>1</sup>Institute of Organic Chemistry with Centre of Phytochemistry, Bulgarian Academy of Sciences, Acad. G. Bonchev str., bl. 9, 1113 Sofia, Bulgaria

<sup>3</sup>Center for Information Science, Kokushikan University, 4-28-1, Setagaya, Setagaya-ku, 154-8515 Tokyo, Japan

Received May 16, 2014; Revised June 17, 2014

*Dedicated to Acad. Dimiter Ivanov on the occasion of his 120<sup>th</sup> birth anniversary*

Time-dependent density functional theory calculations (6-31+G\* basis set) at four functional levels of theory (B3LYP,  $\omega$ B97XD, M06-2X, and PBE0) have been performed in order to estimate their applicability to predict the visible spectra of organic colorants. The absorption wavelength calculations give the following order of performance: M06-2X >  $\omega$ B97XD > PBE0 > B3LYP when set of ionic and neutral dyes is used. In the case of neutral dyes only, the performance at all time-dependent PBE0,  $\omega$ B97XD and M06-2X methods is statistically comparable. The importance of the specific interactions on the  $\lambda_{\max}$  prediction in the case of anionic phenylhydrazone dyes is shown. The comparison between experimental and calculated oscillator strengths was possible only in the case of anthraquinone dyes and has shown that all four methods predict reasonably well the trend of change of the oscillator strength as function of the substituents.

**Key words:** UV-Vis spectra, organic dyes, TD-DFT,  $\omega$ B97XD, M06-2X, PBE0

### INTRODUCTION

A correct prediction of the color (as position of the long-wavelength absorption band, measured as  $\lambda_{\max}$ ) and its intensity (as molar absorptivity of this band and/or the oscillator strength of the corresponding transition) are of crucial importance for the development of new dyes and pigments for traditional and high-technology use [1-3]. During last two decades many attempts to find computational tools that predict the colouristic properties of the most intensively used dyes have been made by applying semi-empirical [4-7] and density functional theory (DFT) [8-12] methods.

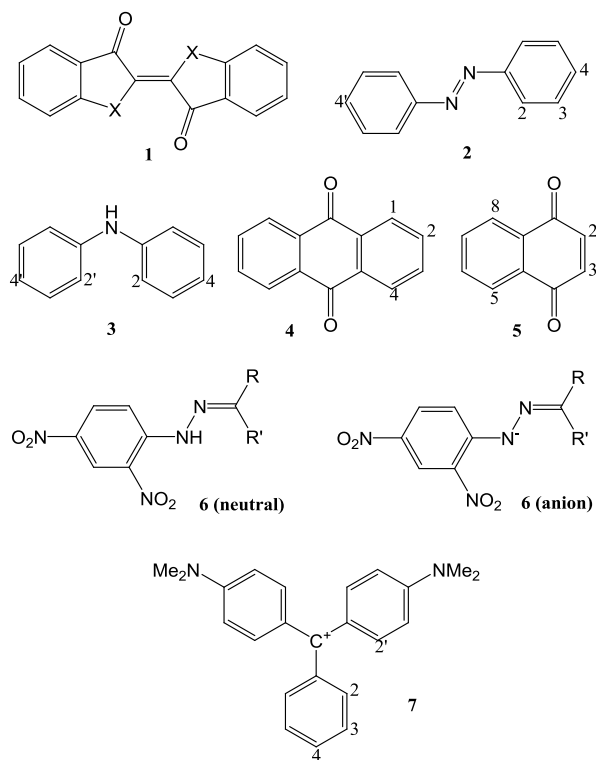
Currently the DFT method [13,14] is the most popular technique for electronic structure calculations with good computational cost/ molecular size ratio, which makes it suitable for electronic structure study of relatively large organic compounds in ground state. The number of the research applications by using time-dependent DFT (TD-DFT) [15] in the prediction of the spectral characteristics in the UV-Vis area is also growing [16,17]. Although its performance in this case had been found mode-

rate for charge-transfer system, which comes as a consequence of the DFT inborn defects, the development of the new functionals tends to improve significantly the situation. Unfortunately, no systematic way for such improvement is known up to now, in contrast to some of the traditional wavefunction-based methods like configuration interaction or coupled cluster theory, and the current approach is to test the TD-DFT results obtained by using various functionals against experimentally measured spectral data ( $\lambda_{\max}$  and in some rare cases - oscillator strengths) of selected organic dyes. In many of the cases direct conclusions about the performance of the different density functionals is impossible, because on one side different basis sets are used and on the other side there is no standardized spectral data set to test on. The most intensively used set of spectral data containing 30 dye structures (neutral and ionized, Scheme 1) had been introduced by Adachi and Nakamura [5] and has been used to estimate the performance of B3LYP and BPW91 [8] functionals. Later, this set has been enlarged to 100 structures by Jacquemin et al. [11], who used them to test five conventional and long-range corrected DFT functionals (PBE, PBE0, LC-PBE, LC- $\omega$ PBE and CAM-B3LYP).

\* To whom all correspondence should be sent:

E-mails: skawauch@polymer.titech.ac.jp (SK) © 2014 Bulgarian Academy of Sciences, Union of Chemists in Bulgaria  
lantonov@orgchm.bas.bg (LA)

Recently, intensive TD-DFT benchmarking (~500 compounds) has been performed using 29 DFT functionals (LDA, GGA, meta-GGA, global and long-range corrected hybrids), showing that any conclusion is strongly dependent on the set of organic molecules selected [18].



**Scheme 1.** Investigated dye structures.

In the present study, we estimate the ability of four DFT functionals (B3LYP [19-22],  $\omega$ B97XD [23], M06-2X [24], and PBE0 [25,26]) to predict the  $\lambda_{\text{max}}$  of organic dyes using a balanced spectral data set of 50 organic dyes (enlarged set of Adachi and Nakamura [5] including neutral and ionic dyes), where special emphasis has been given to find in the literature spectral data in non-polar solvents, when possible, and to avoid the complications of solvent effects description.

## COMPUTATIONAL METHOD

For the current study representative compounds from several classes of dyes have been selected (Scheme 1): indigo (**1**), azobenzene (**2**), diphenylamine (**3**), anthraquinone (**4**), naphthoquinone (**5**), 2,4-dinitrophenylhydrazone (**6**), malachite green cation (**7**). The structural modifications include change of the skeleton atom(s) and/or adding substituent(s) as presented in Tables 1-7.

Initially the structures were built using SPARTAN [27] interface, and then structural relaxation with Merck molecular force field [28] have been performed. This was carried out for each compound in order to determine a global minimum structure among one or more of minimum structures including local minimum structures.

Then, structures were optimized without any restrictions by using Gaussian 09 program suite [29] at four levels of theory, namely B3LYP,  $\omega$ B97XD, M06-2X and PBE0, and then were characterized as true minima by vibrational frequency calculations. In all cases 6-31+G(d) basis set [30] was applied. After the structure optimization, TD-DFT calculations were carried out at the same basis set in order to get straightforward conclusions about the effect of the basis set size on the reliability of the spectral predictions [31]. The largest absorption wavelength (i.e. lowest excitation energy) having more than 0.01 oscillator strength (this avoids in most of the cases the low intensive  $n\text{-}\pi^*$  transitions) is used to compare with the experimental results. In order to model the solvent effect the Polarizable Continuum Model (PCM), using the integral equation formalism variant (IEFPCM [32]), has been used as implemented in Gaussian 09 [24]. The corresponding solvents are listed in Tables 1-7. In the case of the anionic 4,6-dinitrophenylhydrazone dyes (**6a**, **6c**, **6e**) ethanol was used as a solvent, while acetic acid was the solvent medium for the malachite green family **7**.

In the case of the anionic 4,6-dinitrophenylhydrazone dyes (**6a**, **6c**, **6e**) two type of complexes (with  $\text{Na}^+$  and with ethanol molecule) were modeled by optimization in vacuum using 6-31+G\*\* basis set using full counterpoise (CP) method [33,34] to correct the basis set superposition error. The corresponding TD-DFT calculations were carried out at 6-31+G\* basis set at these optimized structures to be comparable with the result for the rest of the calculated dyes. It is worth to be noted that the DFT functionals chosen for this study are hybrid ones obtained by fitting against various training sets of molecules. The B3LYP is one of the most popular and intensively used functionals [18]. The PBE0 functional is also well known [21]. In comparison to them, the functional  $\omega$ B97XD is a range-separated functional, where the switching between DFT and HF exchange is controlled by  $\omega=0.2$ , the short range HF exchange is ~22%, while the long-range one is 100% [19]. It yields high accuracy in thermochemistry, kinetics and noncovalent interactions. The M06-2X functional developed by Zhao and Truhlar [20] is a high-nonlocality functional with doubled amount of nonlocal

exchange (54% HF exchange), parameterized only chemistry, kinetics, and noncovalent interactions. for nonmetals, but reproduces well thermo-

**Table 1.** Indigo dyes: calculated and observed values of  $\lambda_{\max}$  [nm].

Dye		Calculated				Observed	Solvent
		B3LYP	$\omega$ B97XD	M06-2X	PBE0		
1a	X=NH	553	481	483	535	605 [35]	CHCl <sub>3</sub>
1b	X=NMe	586	517	524	569	650 [36]	
1c	X=O	430	364	359	411	420 [37]	

**Table 2.** Azo dyes: calculated and observed values of  $\lambda_{\max}$  [nm].

Dye		Calculated				Observed	Solvent
		B3LYP	$\omega$ B97XD	M06-2X	PBE0		
2a	-	338	302	297	326	317 [38]	C <sub>6</sub> H <sub>12</sub>
2b	2-NH <sub>2</sub>	410	357	354	395	417 [5]	EtOH
2c	3-NH <sub>2</sub>	415	328	324	392	315 [2]	hexane
2d	3-NO <sub>2</sub>	353	301	296	327	317 [6]	hexane
2e	4-Cl	348	308	304	337	324 [6]	C <sub>6</sub> H <sub>12</sub>
2f	4-CN	352	310	306	339	324 [6]	EtOH
2g	4-Me	346	308	303	334	324 [6]	C <sub>6</sub> H <sub>12</sub>
2h	4-NEt <sub>2</sub>	402	347	349	388	407 [39]	C <sub>6</sub> H <sub>12</sub>
2i	4-NEt <sub>2</sub> -4'-NO <sub>2</sub>	472	374	382	444	480 [40]	2-methyl THF
2j	4-NH <sub>2</sub>	374	328	326	361	363 [2]	hexane
2k	4-NHMe	385	335	334	372	380 [2]	C <sub>6</sub> H <sub>12</sub>
2l	4-NMe <sub>2</sub>	397	343	344	383	399 [2]	hexane
2m	4-NMe <sub>2</sub> -4'-NO <sub>2</sub>	465	369	376	437	444 [6]	C <sub>6</sub> H <sub>12</sub>
2n	4-NO <sub>2</sub>	368	314	309	350	329 [6]	hexane
2o	4-OH	354	314	310	342	339 [6]	C <sub>6</sub> H <sub>12</sub>
2p	4-OMe	358	316	312	346	342 [6]	hexane

**Table 3.** Diphenylamino dyes: calculated and observed values of  $\lambda_{\max}$  [nm].

Dye		Calculated				Observed	Solvent
		B3LYP	$\omega$ B97XD	M06-2X	PBE0		
3a	2-NO <sub>2</sub>	451	357	347	416	415 [41]	hexane
3b	4-NO <sub>2</sub>	369	311	313	347	362 [37]	
3c	2,4-diNO <sub>2</sub>	423	343	338	392	411 [37]	

**Table 4.** Anthraquinone dyes: calculated and observed [42] values of  $\lambda_{\max}$  [nm].

Dye		Calculated				Observed	Solvent
		B3LYP	$\omega$ B97XD	M06-2X	PBE0		
4a	1-NH <sub>2</sub>	457	383	378	438	465	CH <sub>2</sub> Cl <sub>2</sub>
4b	1-OH	410	347	340	393	405	
4c	1,2-diOH	436	358	352	418	416	
4d	1,4-diNH <sub>2</sub>	517	447	445	502	550	
4e	1,4-diOH	466	400	394	451	476	
4f	2-NH <sub>2</sub>	428	345	341	407	410	
4g	2-NMe <sub>2</sub>	475	371	370	449	470	

**Table 5.** Naphthoquinone dyes: calculated and observed [43] values of  $\lambda_{\max}$  [nm].

Dye		Calculated				Observed	Solvent
		B3LYP	$\omega$ B97XD	M06-2X	PBE0		
5a	2,3-diCl-5-NH <sub>2</sub> -8-OMe	501	420	416	482	540	C <sub>6</sub> H <sub>12</sub>
5b	5-NH <sub>2</sub>	493	408	400	471	484	
5c	5-NH <sub>2</sub> -8-OMe	499	417	405	480	512	
5d	5-OMe	372	309	300	354	387	

**Table 6.** Neutral and deprotonated hydrazone dyes: calculated and observed [44] values of  $\lambda_{\max}$  [nm].

Dye	Calculated				Observed	Solvent
	B3LYP	$\omega$ B97XD	M06-2X	PBE0		
<b>6a</b> H, H (anion)	501	414	404	466	500	EtOH/NaOH
<b>6b</b> H, H (neutral)	392	331	322	369	345	CHCl <sub>3</sub>
<b>6c</b> <i>p</i> -NH <sub>2</sub> C <sub>6</sub> H <sub>4</sub> , Me (anion)	539	427	419	500	461	EtOH/NaOH
<b>6d</b> <i>p</i> -NH <sub>2</sub> C <sub>6</sub> H <sub>4</sub> , Me (neutral)	510	366	366	465	403	CHCl <sub>3</sub>
<b>6e</b> <i>p</i> -NO <sub>2</sub> C <sub>6</sub> H <sub>4</sub> , Me (anion)	601	484	501	566	540	EtOH/NaOH
<b>6f</b> <i>p</i> -NO <sub>2</sub> C <sub>6</sub> H <sub>4</sub> , Me (neutral)	435	349	344	403	382	CHCl <sub>3</sub>

**Table 7.** Malachite green dyes: calculated and observed [45-48] values of  $\lambda_{\max}$  [nm].

Dye	Calculated				Observed	Solvent
	B3LYP	$\omega$ B97XD	M06-2X	PBE0		
<b>7a</b> None	489	448	460	476	621	
<b>7b</b> 2-NO <sub>2</sub>	502	461	474	487	637	
<b>7c</b> 2-OMe	496	454	468	482	625	
<b>7d</b> 2,2'-diMe	499	460	473	487	634	
<b>7e</b> 3-OMe	506	449	461	482	623	
<b>7f</b> 4-Cl	493	451	463	480	628	
<b>7g</b> 4-CN	505	460	472	492	643	
<b>7h</b> 4-Me	488	445	458	475	617	
<b>7i</b> 4-NO <sub>2</sub>	516	463	476	499	645	
<b>7j</b> 4-OH	487	441	454	474	603	
<b>7k</b> 4-OMe	487	439	453	474	608	98% acetic acid

## RESULTS AND DISCUSSION

The predicted band positions in vacuum are compared with the experimental ones in Tables 1-7 and the overall performance of the used TD-DFT methods is shown in Fig. 1.

The visual inspection of Fig. 1 allows several interesting conclusions to be pointed out. In the case of TD-B3LYP and TD-PBE0 there are obvious correlation trends where compounds **6c**, **6e** and **6d**, and the whole class of dyes **7**, i.e., Malachite green dyes, are outliers. In the case of TD- $\omega$ B97XD and TD-M06-2X the Malachite green dyes are part of the linear tendency, while **6c** and **6e** remain, to a certain extent, deviated from the relation along with **5d**. Visually the performance of TD- $\omega$ B97XD and TD-M06-2X is better than the TD-B3LYP and TD-PBE0.

The statistical information collected in Table 8 support these initial conclusions.

The statistical analysis, comparing predicted and experimentally observed  $\lambda_{\max}$ , shows substantially lower mean average errors in the cases of B3LYP and PBE0. This is not in contradiction with Fig. 1 since these two methods do not give systematical shift of the predicted band positions, i.e. there are large negative and positive deviations, which at end

neutralize each other. According to the deviations given in Table 8, the observed values for **7** are underestimated by the calculations (largest positive deviations are 138 nm and 151 nm for B3LYP and PBE0 respectively, both in the case of **7g**), while the band positions for the anionic dyes are overestimated (with 107 nm for TD-B3LYP and 64 nm for TD-PBE0, both in the case of **6d**).

The TD- $\omega$ B97XD and TD-M06-2X calculated  $\lambda_{\max}$  quantities are systematically deviated, underestimating the experiment, which leads to larger mean absolute error (MAE) and root mean square (RMS) values. However, according to our results and the previously published prediction of band positions by various DFT functionals [9-12] there is no DFT method that directly predict the real band positions, i.e. there is inherent problem associated with the TD calculation with the hybrid DFT methods.

The practical solution is to find a DFT method whose predictions correlate with the experiment and to use this correlation for additional correction of the calculated  $\lambda_{\max}$  values. Actually this has been performed and the linear regression parameters are collected in Table 8. In the ideal case the linear fit coefficients *a* and *b* must tend to 1 and 0

respectively, but as we mentioned above the tested functionals do not directly predict experimentally observed band positions. The data in Table 8 show very clearly that  $\omega$ B97XD and M06-2X results correlate very satisfactory with the experiment and substantially better than those of B3LYP and PBE0. This leads to substantially lower MAE and RMS values and narrow limits of the maximal positive and negative deviations. As seen after the fitting the Malachite green dyes remain problematic for B3LYP, while in the case of the rest three DFT methods largest positive deviation is obtained at **5d**.

The anionic dyes also remain problematic, but in smaller extent for M06-2X.

Taking into account the all statistical data we can conclude that the order of performance of the tested four functionals is as follows: M06-2X> $\omega$ B97XD>PBE0>B3LYP. According to the recent data of Jacquemin et al. [11], obtained with 6-311+G(2d,p) basis set (at PBE0/6-311G\*\* geometry), the performance of their tested functionals with a set of 100 neutral dyes follows the PBE>PBE0>CAM-B3LYP>LC-PBE>LC- $\omega$ PBE>HF sequence. Since the used sets of dyes overlap and although the used basis sets are different we

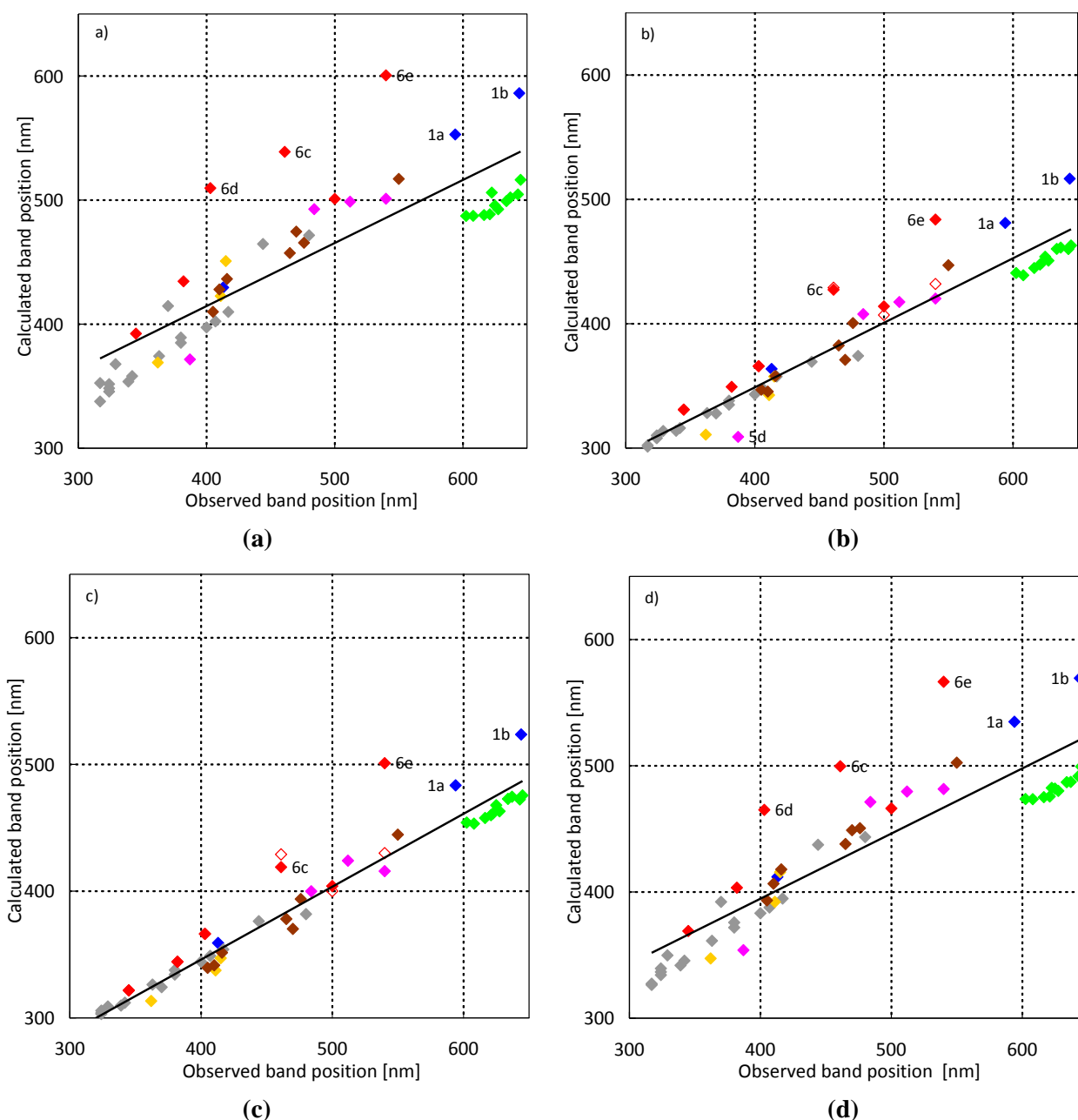


**Fig. 1.** Comparison between calculated (in vacuum) and experimental band positions at: a) B3LYP; b)  $\omega$ B97XD; c) M06-2X; d) PBE0. The families of dyes are presented as following colors: **1** – blue; **2** – grey; **3** – orange; **4** – brown; **5** – pink; **6** – red; **7** – green. The calculated values for the complexes of **6a,c,e** with  $\text{Na}^+$  are given with empty symbols.

**Table 8.** Statistical analysis of the prediction capacity in vacuum and in solution (underlined). The corresponding values obtained by taking into account the interaction between anionic phenylhydrazone dyes and Na<sup>+</sup> are presented in curly brackets.

Parameter	B3LYP	$\omega$ B97XD	M06-2X	PBE0
<i>without fit</i>				
MAE* [nm]	47 <u>52</u>	83 {84} <u>63 {65}</u>	82 {83} <u>63 {64}</u>	48 <u>44</u>
RMS** [nm]	69 <u>65</u>	99 {100} <u>81 {81}</u>	96 {97} <u>76 {77}</u>	71 <u>59</u>
largest positive deviation*** [nm]	138 ( <b>7g</b> ) <u>106 (<b>7d</b>)</u>	183 ( <b>7g</b> ) <u>148 (<b>7g</b>)</u>	171 ( <b>7g</b> ) <u>133 (<b>7g</b>)</u>	151 ( <b>7g</b> ) <u>116 (<b>7d</b>)</u>
largest negative deviation [nm]	-107 ( <b>6d</b> ) <u>-169 (<b>6d</b>)</u>	- <u>-7 (<b>6c</b>)</u>	- <u>-</u>	-62 ( <b>6d</b> ) <u>-108 (<b>6c, 6d</b>)</u>
<i>with correction equation**** <math>a \cdot \lambda_{calc} - b</math>, obtained by linear fit between <math>\lambda_{obs}</math> and <math>\lambda_{calc}</math></i>				
<i>a</i>	1.968 <u>1.704</u>	1.927 {1.953} <u>1.724 {1.736}</u>	1.739 {1.767} <u>1.560 {1.572}</u>	1.938 <u>1.724</u>
<i>b</i>	415 <u>348</u>	293 {279} <u>228 {231}</u>	202 {210} <u>162 {165}</u>	364 <u>317</u>
R <sup>2</sup>	0.712 <u>0.672</u>	0.917 {0.936} <u>0.929 {0.940}</u>	0.936 {0.955} <u>0.947 {0.954}</u>	0.785 <u>0.773</u>
MAE [nm]	56 <u>59</u>	23 {20} <u>20 {18}</u>	18 {16} <u>18 {16}</u>	46 <u>45</u>
RMS [nm]	70 <u>77</u>	33 {29} <u>30 {28}</u>	29 {24} <u>26 {24}</u>	57 <u>59</u>
largest positive deviation [nm]	76 ( <b>7a</b> ) <u>85 (<b>7h</b>)</u>	64 ( <b>5d</b> ) <u>66 (<b>5d</b>)</u>	67 ( <b>5d</b> ) <u>67 (<b>5d</b>)</u>	66 ( <b>5d</b> ) <u>76 (<b>5d</b>)</u>
largest negative deviation [nm]	-226 ( <b>6e</b> ) <u>-258 (<b>6c</b>)</u>	-120 ( <b>6e</b> ) <u>-119 (<b>6c</b>)</u>	-129 ( <b>6e</b> ) <u>-94 (<b>6c</b>)</u>	-193 ( <b>6e</b> ) <u>-204 (<b>6c</b>)</u>

\* mean absolute error; \*\* root mean square; \*\*\* deviations are calculated as difference between observed and calculated band position, namely:  $\lambda_{obs} - \lambda_{calc}$ ; in this case the statistical analysis (MAE, RMS and deviations) is based on comparison between  $\lambda'_{calc}$  ( $\lambda'_{calc} = a \cdot \lambda_{calc} + b$ ) and  $\lambda_{obs}$ .

can conclude that M06-2X method could be used for practical prediction of the experimental spectra of organic dyes. The exclusion of the ionic dyes (**6** and **7**) from the linear fitting leads to correlation (R<sup>2</sup>) 0.9725, 0.9530 and 0.9690 for TD-PBE0, TD- $\omega$ B97XD and TD-M06-2X respectively, which means that these three methods are comparable in the case of neutral dyes, but the M06-2X performs much better (Table 8) when ionic dyes are included.

According to Table 8 and Fig. 2 the introduction of the solvent effect does not improve substantially the performance of the tested functionals, even in two of them (B3LYP and PBE0) decrease of the correlation is observed. Generally the solvent inclusion leads to decrease of both slope and intercept of the liner fit, but the systematic deviation in the case of ionic dyes remain unaffected (Fig. 2).

As seen from Fig. 1b,c and 2b,c in the case of  $\omega$ B97XD and M06-2X functionals the anionic dyes of phenylhydrazone family are substantially deviated from the linear tendency and the situation is practically not affected by introducing solvent environment. This means that the effects are either systematically related to DFT performance or rela-

ted to specific, intermolecular, effects in solution. Compounds **6b**, **6d** and **6f** are treated with NaOH in ethanol solution to give the deprotonated species **6a**, **6c** and **6e**, resp., which could lead to hypothesis for specific interaction with Na<sup>+</sup> or with ethanol molecule. According to the calculations, the optimized complexes with Na<sup>+</sup> have shown much more stability in both vacuum and solvent field in all three anionic dyes comparing to the corresponding ethanol complexes. As seen from Fig. 1 and 2 the use of the Na complexes of the anionic phenylhydrazones leads to some improvement of the overall performance, but it does not substantially changes the overall statistical parameters (as shown in Table 8). Evidently latter comes from the fact that the three anionic dyes have negligible weight in the whole set of 50 compounds.

As it was mentioned before, the prediction of the band position is only one side of the overall color/properties elucidation. The real dye development needs information for the intensity of the color in the same extend, or even in larger, as the information for the long-wavelength band position. Such information is provided by the TD-DFT as

oscillator strength ( $f$ ), which fundamental value defines how probable is the corresponding transition [49].

The corresponding values for the studied dyes and the used DFT functionals are available from the authors upon request. Unfortunately in most of the cases there is no way for direct comparison with the experiment. Where available, the experimental data are presented as molar absorptivity ( $\epsilon_{\max}$ ) at  $\lambda_{\max}$ . The fundamental relation between  $f$  and  $\epsilon_{\max}$  is well known:

$$f \cong 4.39 \cdot 10^{-9} \cdot \int \epsilon(\tilde{\nu}) d\tilde{\nu}$$

where the spectrum must be presented in wave numbers ( $\tilde{\nu}$ ). If the spectral band is individual (resolved mathematically [50] or experimentally) and its shape is assumed to be Gaussian function [29,30], as it is in UV-Vis spectra, the integral band can be presented as follows:

$$\int \epsilon(\tilde{\nu}) d\tilde{\nu} = 1.063 \cdot \epsilon_{\max}^o \cdot \Delta\tilde{\nu}_{1/2}$$

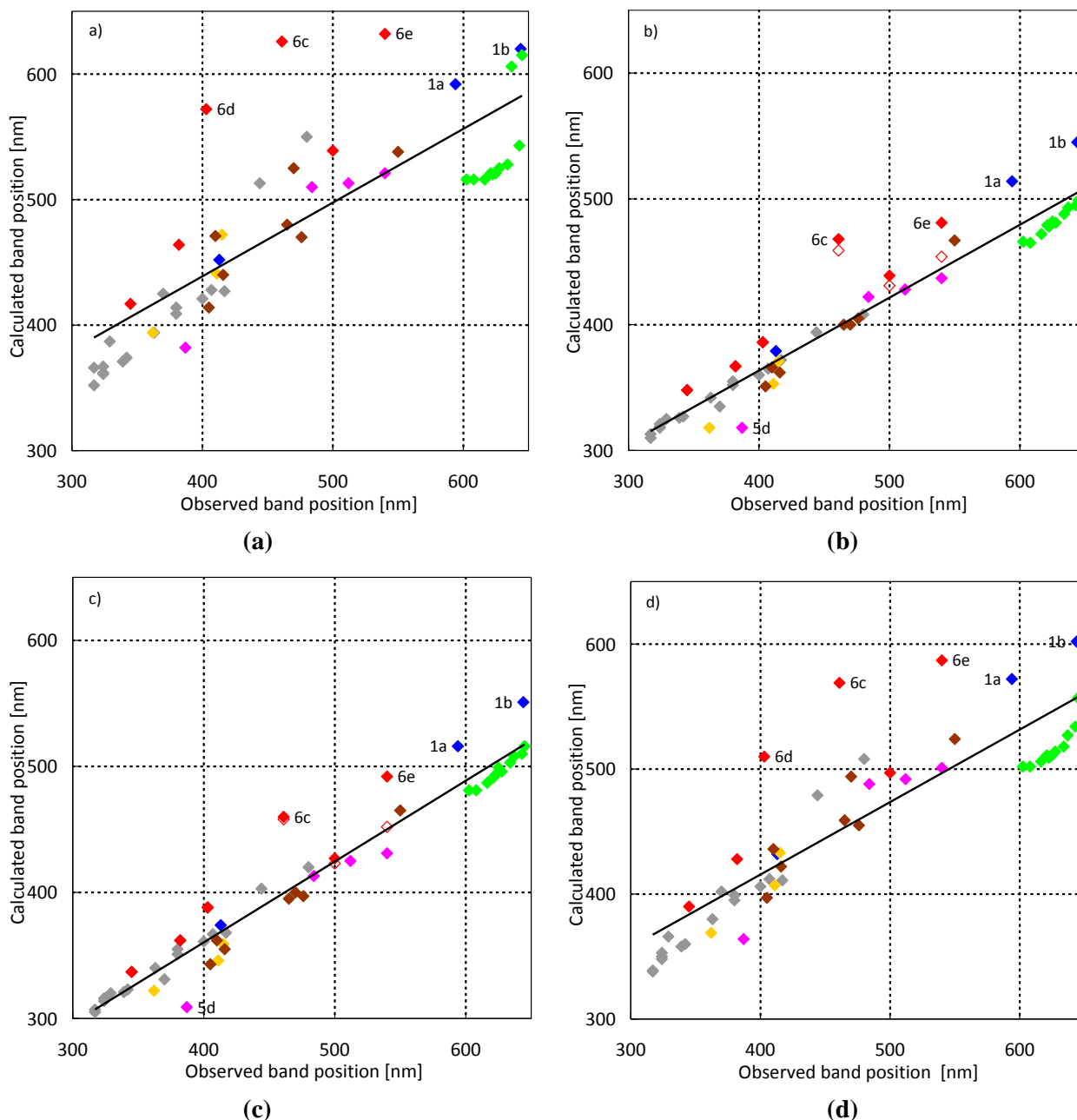


**Fig. 2.** Comparison between calculated (in corresponding solvents) and experimental band positions at: a) B3LYP; b)  $\omega$ B97XD; c) M06-2X; d) PBE0. The families of dyes are presented as following colors: 1 – blue; 2 – grey; 3 – orange; 4 – brown; 5 – pink; 6 – red; 7 – green. The calculated values for the complexes of **6a,c,e** with  $\text{Na}^+$  are given with empty symbols.

**Table 9.** Anthraquinone dyes: calculated and observed [38] oscillator strengths.

Dye	Calculated				Observed	
	B3LYP	$\omega$ B97XD	M06-2X	PBE0		
<b>4a</b>	1-NH <sub>2</sub>	0.119	0.1692	0.1595	0.128	0.114
<b>4b</b>	1-OH	0.1238	0.1737	0.1621	0.1334	0.113
<b>4c</b>	1,2-diOH	0.0952	0.1495	0.1342	0.1052	0.119
<b>4d</b>	1,4-diNH <sub>2</sub>	0.1866	0.235	0.2242	0.1988	0.157
<b>4e</b>	1,4-diOH	0.1727	0.2263	0.213	0.1848	0.131
<b>4f</b>	2-NH <sub>2</sub>	0.0495	0.0742	0.0762	0.0488	0.091
<b>4g</b>	2-NMe <sub>2</sub>	0.07	0.1096	0.1117	0.0773	0.109

Depending on the extent of band overlapping in the visible area (which is usually substantial) the experimental maximal molar absorptivity ( $\epsilon_{\max}$ ) differs from the individual one ( $\epsilon_{\max}^o$ ). In addition there is no way of estimation of the band width ( $\Delta\tilde{\nu}_{1/2}$ ) from the experimental spectrum without resolving it mathematically [29]. For these reasons, assuming a universal value for the band width of  $4000\text{ cm}^{-1}$  as it was made [8] does not have physical meaning and finally cannot bring any conclusions.

In the experimental dye set used by us the experimentally determined oscillator strengths are available for the anthraquinone dyes **4** (Table 9), which allows a direct comparison. This comparison shows that the DFT methods tested in this study correctly predict the tendency (with statistically comparable correlation in all four cases), but the data are not sufficient to make statistically valid conclusions about the overall performance.

## CONCLUSION

TD-DFT calculations with 6-31+G\* basis set at four functional levels of theory, namely B3LYP,  $\omega$ B97XD, M06-2X, and PBE0, have been performed in order to estimate their applicability to predict the visible spectra of organic colorants. For this purpose a set of 50 dye structures, including ionic and neutral, has been used. It has been found that there are good correlation relationships between the calculated wavelength values and the observed wavelength values. The absorption wavelength calculations at the M06-2X and  $\omega$ B97XD functional levels were found to provide better prediction than those at the B3LYP and PBE0 functional levels. Comparing our data and data, previously published by other authors, we can conclude that M06-2X could be recommended for predicting visible spectra of organic dyes. The use of solvent effect description (as PCM) leads also to improvement of the results.

The comparison between experimental and calculated oscillator strengths was possible only in the case of anthraquinone dyes and has shown that all four methods predict reasonably well the trend of change of the oscillator strength.

This study has shown that there is need for establishment of a standard set of dyes (as structures with colors equally distributed through the visible area and strictly determined oscillator strengths), which to be used for comparative testing of various methods and basis sets.

**Acknowledgements:** LA is indebted to JSPS for the fellowship provided. The numerical calculations were carried out on the TSUBAME2.5 supercomputer at the Tokyo Institute of Technology, Tokyo, Japan, and on the supercomputer at the Research Center for Computational Science, Okazaki, Japan.

## REFERENCES

1. H. Zollinger, *Color - A Multidisciplinary Approach*, Wiley-VCH, Weinheim, 1999.
2. J. Fabian, H. Hartmann, *Light Absorption of Organic Colorants: Theoretical Treatment and Empirical Rules*, Springer-Verlag, Berlin, 1980.
3. J. Griffiths, *Colour and Constitution of Organic Molecules*, Academic Press, London, 1976.
4. C. Forber, E. Kelusky, N. Bunce, M. Zerner, *J. Am. Chem. Soc.*, **107**, 5884 (1985).
5. M. Adachi, S. Nakamura, *Dyes Pigm.*, **17**, 287 (1991).
6. A. Matsuura, H. Sato, W. Sotoyama, A. Takahashi, M. Sakurai, *J. Mol. Struct.: Theochem*, **860**, 119 (2008).
7. S. Kawauchi, K. Mita, M. Satoh, J. Komiyama, J. Watanabe, Y. Tamura, K. Mori, K. Suzuki, *Nonlinear Optics*, **26**, 221 (2000).
8. D. Guillaumont, S. Nakamura, *Dyes Pigm.*, **46**, 85 (2000).
9. P. C. Chen, Y. C. Chieh, J. C. Wu, *J. Mol. Struct.: Theochem*, **715**, 183 (2005).
10. C. Adamo, D. Jacquemin, *Chem. Soc. Rev.*, **42**, 845 (2013).

11. A. D. Laurent, D. Jacquemin, *Int. J. Quant. Chem.*, **17**, 2019 (2013).
12. D. Jacquemin, J. Preat, E. A. Perpète, D. P. Vercauteren, J.-M. Andre, I. Ciofini, C. Adamo, *Int. J. Quant. Chem.*, **111**, 4224 (2011).
13. P. Hohenberg, W. Kohn, *Phys. Rev.*, **136B**, 864 (1964).
14. W. Kohn, L. J. Sham, *Phys. Rev.*, **140**, A1133 (1965).
15. R. E. Stratman, G. E. Scuseria, M. J. Frisch, *J. Chem. Phys.*, **109**, 8218 (1998).
16. B. Mennucci Computational Spectroscopy, Ed. J. Grunenberg, Wiley-VCH, Weinheim, 2010, pp. 151-168.
17. P. H. P. Harbach, A. Dreuw, Modeling of Molecular Properties, ed. by P. Comba, Wiley-VCH, Weinheim, 2011, pp. 29-45.
18. D. Jacquemin, V. Watherlet, E. A. Perpète, G. E. Scuseria, C. Adamo, *J. Chem. Theory Comput.*, **5**, 2420 (2009) and the references cited therein in respect of the available training sets.
19. A. D. Becke, *J. Chem. Phys.*, **98**, 5648 (1993).
20. C. Lee, W. Yang, R.G. Parr, *Phys. Rev.*, **37B**, 785 (1988).
21. S. H. Vosko, L. Wilk, M. Nusair, *Can. J. Phys.*, **58**, 1200 (1980).
22. P. J. Stephens, F. J. Devlin, C. F. Chabalowski, M. J. Frisch, *J. Phys. Chem.*, **98**, 11623 (1994).
23. J.-D. Chai, M. Head-Gordon, *Phys. Chem. Chem. Phys.*, **10**, 6615 (2008).
24. Y. Zhao, D. G. Truhlar, *Theor. Chem. Acc.*, **120**, 215 (2008).
25. J. P. Perdew, K. Burke, M. Ernzerhof, *Phys. Rev. Lett.*, **77**, 3865 (1996).
26. C. Adamo, V. Barone, *J. Chem. Phys.*, **110**, 6158 (1999).
27. Y. Shao, L.F. Molnar, Y. Jung, J. Kussmann, C. Ochsenfeld, *Phys. Chem. Chem. Phys.*, **8**, 3172 (2006).
28. T. A. Halgren, *J. Comp. Chem.*, **17**, 490 (1996).
29. M. J. Frisch, G. W. Trucks, H. B. Schlegel, G. E. Scuseria, M. A. Robb, J. R. Cheeseman, G. Scalmani, V. Barone, B. Mennucci, G. A. Petersson, H. Nakatsuji, M. Caricato, X. Li, H. P. Hratchian, A. F. Izmaylov, J. Bloino, G. Zheng, J. L. Sonnenberg, M. Hada, M. Ehara, K. Toyota, R. Fukuda, J. Hasegawa, M. Ishida, T. Nakajima, Y. Honda, O. Kitao, H. Nakai, T. Vreven, J. A. Montgomery, Jr., J. E. Peralta, F. Ogliaro, M. Bearpark, J. J. Heyd, E. Brothers, K. N. Kudin, V. N. Staroverov, R. Kobayashi, J. Normand, K. Raghavachari, A. Rendell, J. C. Burant, S. S. Iyengar, J. Tomasi, M. Cossi, N. Rega, J. M. Millam, M. Klene, J. E. Knox, J. B. Cross, V. Bakken, C. Adamo, J. Jaramillo, R. Gomperts, R. E. Stratmann, O. Yazyev, A. J. Austin, R. Cammi, C. Pomelli, J. W. Ochterski, R. L. Martin, K. Morokuma, V. G. Zakrzewski, G. A. Voth, P. Salvador, J. J. Dannenberg, S. Dapprich, A. D. Daniels, O. Farkas, J. B. Foresman, J. V. Ortiz, J. Cioslowski, D. J. Fox, Gaussian 09, Revision A.02, Gaussian, Inc., Wallingford CT, 2009.
30. J. S. Binkley, J. A. Pople, W. J. Hehre, *J. Am. Chem. Soc.*, **102**, 939 (1980).
31. R. Improta, UV-Visible Absorption and Emission Energies in Condensed Phase by PCM/TD-DFT Methods, in Computational Strategies for Spectroscopy, V. Barone (Ed.), Wiley-VCH, Weinheim, 2012.
32. J. Tomasi, B. Mennucci, R. Cammi, *Chem. Rev.*, **105**, 2999 (2005).
33. S. B. Boys, F. Bernardi, *Mol. Phys.*, **19**, 553 (1970).
34. S. Simon, M. Duran, J. J. Dannenberg, *J. Chem. Phys.*, **105**, 11024 (1996).
35. W. R. Brode, E. G. Pearson, G. M. Wyman, *J. Am. Chem. Soc.*, **76**, 1034 (1954).
36. R. Pummerer, G. Marondel, *Liebigs Ann. Chem.*, **602**, 228 (1957).
37. R. Pummerer, G. Marondel, *Chem. Ber.*, **93**, 2834 (1960).
38. S. Yamamoto, N. Nishimura, S. Hasegawa, *Bull. Chem. Soc. Jpn.*, **44**, 2018 (1971).
39. H. Mustroph, *Dyes Pigm.*, **15**, 129 (1991).
40. S. Lunak Jr., M. Nepas, R. Hrdina, H. Mustroph, *Chem. Phys.*, **184**, 255 (1994).
41. M. G. W. Bell, M. Day, A. T. Peters, *J. Soc. Dyers Colour.*, **82**, 410 (1966).
42. H. Labhart, *Helv. Chim. Acta*, **40**, 1410 (1957).
43. K.-Y. Chu, J. Griffiths, *J. Chem. Res. (S)*, 180 (1978).
44. L. A. Jones, C. K. Hancock, *J. Org. Chem.*, **25**, 226 (1960).
45. C. C. Barker, M. H. Bride, G. Hallas, A. Stamp, *J. Chem. Soc.*, 1285 (1961).
46. C. C. Barker, G. Hallas, *J. Chem. Soc.*, 1529 (1961).
47. A. S. Ferguson, G. Hallas, *J. Soc. Dyers Colour.*, **87**, 187 (1971).
48. A. S. Ferguson, G. Hallas, *J. Soc. Dyers Colour.*, **89**, 22 (1973).
49. L. Antonov, D. Nedeltcheva, *Chem. Soc. Rev.*, **29**, 217 (2000).
50. L. Antonov, S. Stoyanov, *Appl. Spectrosc.*, **47**, 1030 (1993).

## ПРЕДСКАЗВАНЕ НА ЦВЕТА НА БАГРИЛА ПОСРЕДСТВОМ ЗАВИСЕЩА ОТ ВРЕМЕТО ТЕОРИЯ НА ФУНКЦИОНАЛА НА ПЛЪТНОСТТА (TD-DFT)

С. Каваучи<sup>1\*</sup>, Л. Антонов<sup>1,2\*</sup>, И. Окуно<sup>3</sup>

<sup>1</sup>*Департамент по Органични и полимерни материали, Токийски Технологичен институт, 152-8552 Токио, Япония*

<sup>2</sup>*Институт по Органична химия с Център по Фитохимия, Българска Академия на Науките, ул. Акад. Г. Бончев, бл. 9, 1113 София, България*

<sup>3</sup>*Център по Информационни науки, Университет Кокушикан, 154-8515 Токио, Япония*

Постъпила на 16 май 2014 г.; Коригирана на 17 юни 2014 г.

(Резюме)

Беше проверена приложимостта на четири TD-DFT метода (B3LYP,  $\omega$ B97XD, M06-2X, and PBE0) при базичен набор 6-31+G\* за предсказване на спектрите на органични багрила във видимата област на спектъра. При използване на набор от неутрални и йонни багрила най-добри резултати за положението на дълго-вълновите спектрални максимуми са получени в реда M06-2X> $\omega$ B97XD>PBE0>B3LYP. При използване само на неутрални багрила трите метода, PBE0,  $\omega$ B97XD и M06-2X, показват статистически сравними резултати. При фенилхидразоновите багрила е показана важноста на специфичните взаимодействия в разтвор върху коректното предсказване на  $\lambda$ max. Сравнението на експериментално наблюдаваните и предсказаните сили на осцилатора, което беше възможно само при серията антрахинонови багрила, показа, че и четирите метода предсказват добре общата тенденция на промяна като функция от ефекта на заместителите.